Tuning the redox properties of metalloporphyrin- and metallophthalocyanine-based molecular electrodes for the highest electrocatalytic activity in the oxidation of thiols

Fethi Bedioui,[a] Sophie Griveau,[a] Tebello Nyokong,[b] A. John Appleby,[c] Claudia A. Caro,[d] Miguel Gulppi,†[e] Gonzalo Ochoa[e] and José H. Zagal*[e]

Received 22nd December 2006, Accepted 14th March 2007
First published as an Advance Article on the web 11th April 2007
DOI: 10.1039/b618767f

In this work we discuss different approaches for achieving electrodes modified with N_4 macrocyclic complexes for the catalysis of the electrochemical oxidation of thiols. These approaches involve adsorption, electropolymerization and molecular anchoring using self assembled monolayers. We also discuss the parameters that determine the reactivity of these complexes. Catalytic activity is associated with the nature of the central metal, redox potentials and Hammett parameters of substituents on the ligand. Correlations between catalytic activity (log *i* at constant *E*) and the redox potential of catalysts for complexes of Cr, Mn, Fe, Co, Ni and Cu are linear with an increase of activity for more positive redox potentials. For a great variety complexes bearing the same metal center (Co) correlations between log *i* and $E^{o\prime}$ of the Co(II)/Co(I) couple have the shape of an unsymmetric volcano. This indicates that the potential of the Co(II)/Co(I) couple can be tuned using the appropiate ligand to achieve maximum catalytic activity. Maximum activity probably corresponds to a ΔG of adsorption of the thiol on the Co center equal to zero, and to a coverage of active sites by the thiol equal to 0.5.

1. Introduction

Metal complexes of N_4-ligands, MN_4, such as metalloporphyrins (MP), metalloporphyrazines (also called tetraazaporphyrins) and phthalocyanines (MPc) are of great technological importance and fundamental interest. Their structure is similar to that of biological molecules such as haemoglobin, chlorophyll, and cyanocobalamine (vitamin B_{12}) and they have attracted considerable interest because of their biological relevance and their technological applications are very broad.[1–30] They are well known as catalysts for both homogeneous and heterogeneous chemical reactions[1–5] and in most cases, these reactions involve the transfer of electrons. This makes these complexes a promising class of catalysts as they provide very interesting models for theoretical and experimental studies. Also, their catalytic action can be finely tuned through their chemical structure. Fig. 1 and 2 illustrate the structures of some metalloporphyrins and metallophthalocyanines that have been studied for their electrocatalytic properties.

[a] *INSERM, U 640, CNRS, UMR 8151, École Nationale Supérieure de Chimie de Paris, René Descartes Paris 5, Chemical and Genetic Pharmacology Laboratory, Paris, France*
[b] *Department of Chemistry, Rhodes University, Grahamstown, South Africa*
[c] *Center for Electrochemical Systems and Hydrogen Research 3402 Texas A & M University, College Station, TX, 77843, USA*
[d] *Facultad de Ciencias, Departamento de Ciencias Básicas, Universidad del Bío-Bío, Chillán, Chile*
[e] *Departamento de Química de los Materiales, Facultad de Química y Biología, Universidad de Santiago de Chile, Casilla 40, Correo 33 Santiago, Chile*
† Present address: Biosigma S. A. Santiago, Chile.

Besides the wide development of MP and MPc complexes in fundamental research devoted to biomimetic catalysis,[30–33] they are largely involved in industrial applications that include energy conversion,[7–9] semiconductor devices,[10,11] photosensitizers,[12] chemical sensors,[13,14] electrophotography,[15] gas sensors,[16] electrochromic devices,[17] solar cells,[18] optoelectronic devices,[19] liquid crystals,[20] low dimensional metals,[21,22] Langmuir-Blodgett films[23] catalysts and electrocatalysts.[7,24–30,33,34] In the latter case, these complexes are deposited onto electrode surfaces by several ways to form what is called "molecular porphyrin or phthalocyanine electrodes".

In the last decades, several studies have reported on MP and MPc and related complexes that exhibit catalytic activity for electrochemical oxidation of a variety of thiols[29,35–63] and for the reduction of the corresponding disulfides.[63] Thus, "molecular porphyrin and phthalocyanine electrodes" act as electrocatalysts, by lowering particularly the overpotential of oxidation or reduction of the target molecules.[29] Reported studies related to the electro-oxidation of thiols to give the corresponding disulfides have shown that the catalytic activity of the molecular electrodes strongly depends on the nature of the central metal, with cobalt derivatives giving the best results.[29] On the other hand, the rates of the electrochemical oxidation of thiols are strongly dependent of the nature of the N_4-macrocycle ligand.

The electrocatalytic oxidation of thiols can be considered as an inner-sphere reaction since a strong interaction between a sulfur atom and an active site is expected to occur before or when the electron transfer takes place.[29] In some cases, this interaction is so strong that the catalytic process is inhibited as the active sites are blocked by adsorbed species. Indeed, in the

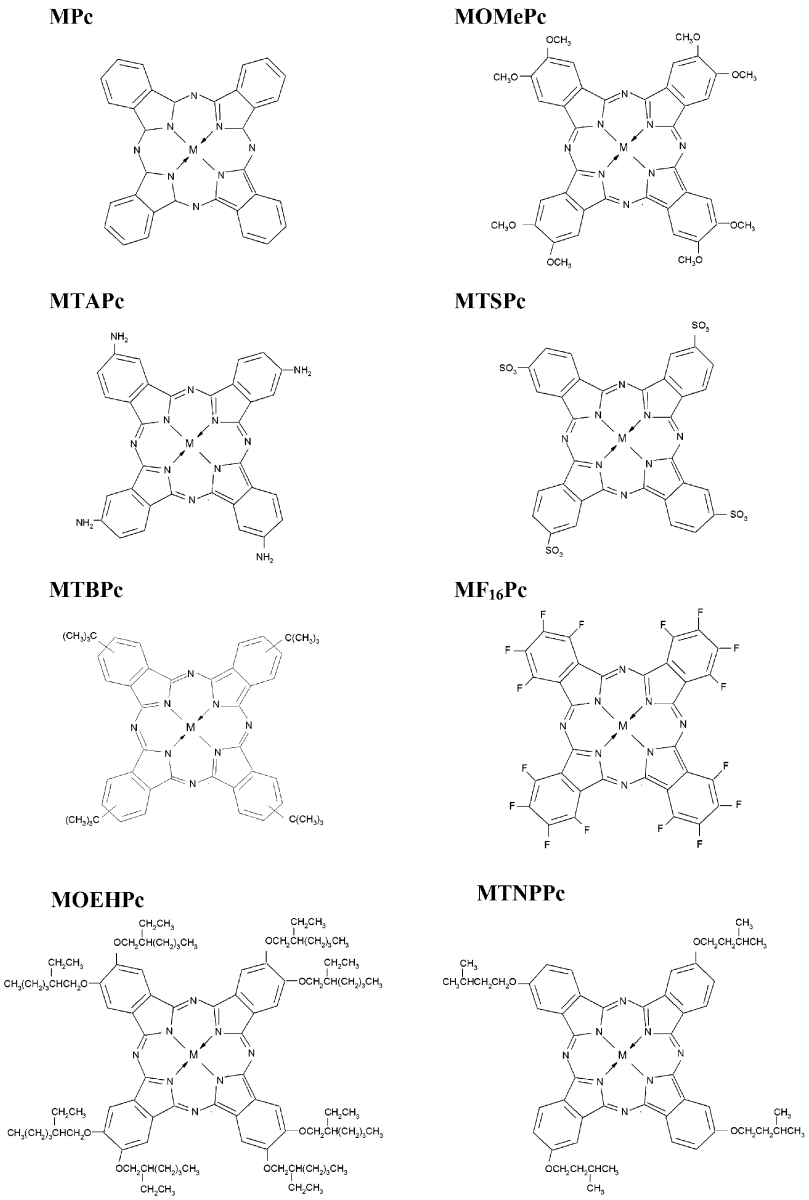

Fig. 1 Structures of the metallophthalocyanines bearing different substituents: MPc metallo-phthalocyanine; MOMePc metallo-octamethoxyphthalocyanine; MTAPc metallo-tetraaminophthalocyanine; MTSPc metallo-tetrasulfophthalocyanine; MTBPc metallo-tetra-*tert*-butylphthalocyanine; $MF_{16}Pc$ metallo-hexadecafluorophthalocyanine; MOEHPc metallo-octaethylhexyloxyphthalocyanine; MTNPPc metallo-tetraneopentoxyphthalocyanine.

case of polytetraaminocobalt phthalocyanine deposited on transparent ITO electrodes, there is *in situ* evidence that an adduct can be formed between this molecule and 2-mercaptoethanol (2-ME).[45,52] This adduct could be a precursor in the electrocatalytic oxidation of thiols. Also, electroreflectance spectroscopy studies on Co and Fe tetrasulfonated phthalocyanines adsorbed on the basal plane of highly oriented pyrolytic graphite electrodes have demonstrated that under open-circuit conditions, in basic deaerated aqueous solutions, L-cysteine reduces the metal in the adsorbed phthalocyanine from M(II) to M(I)[46] suggesting that the M(II)/M(I) redox couple in the phthalocyanine plays a role in the catalytic process.

Over the years we have found that the electrocatalytic activity of MP and MPc for the oxidation of thiols such as 2-mercaptoethanol, and 2-aminoethanethiol[49,50,53,62] follows linear correlations with the redox potential (driving force) of the complex, when immobilized on graphite electrodes. It has been found that the activity increases as the M(II)/M(I) formal potential of the catalyst becomes more negative. For the reduction of 2-mercaptodisulfide the activity also increases as the Co(II)/Co(I) becomes more negative.[64] However, it is believed that if a wide enough potential window using different catalysts is chosen, the complete correlation follows a volcano-shape or parabolic curve, as observed for the oxidation of hydrazine.[65,66] Indeed, for the oxidation of 2-ME when five

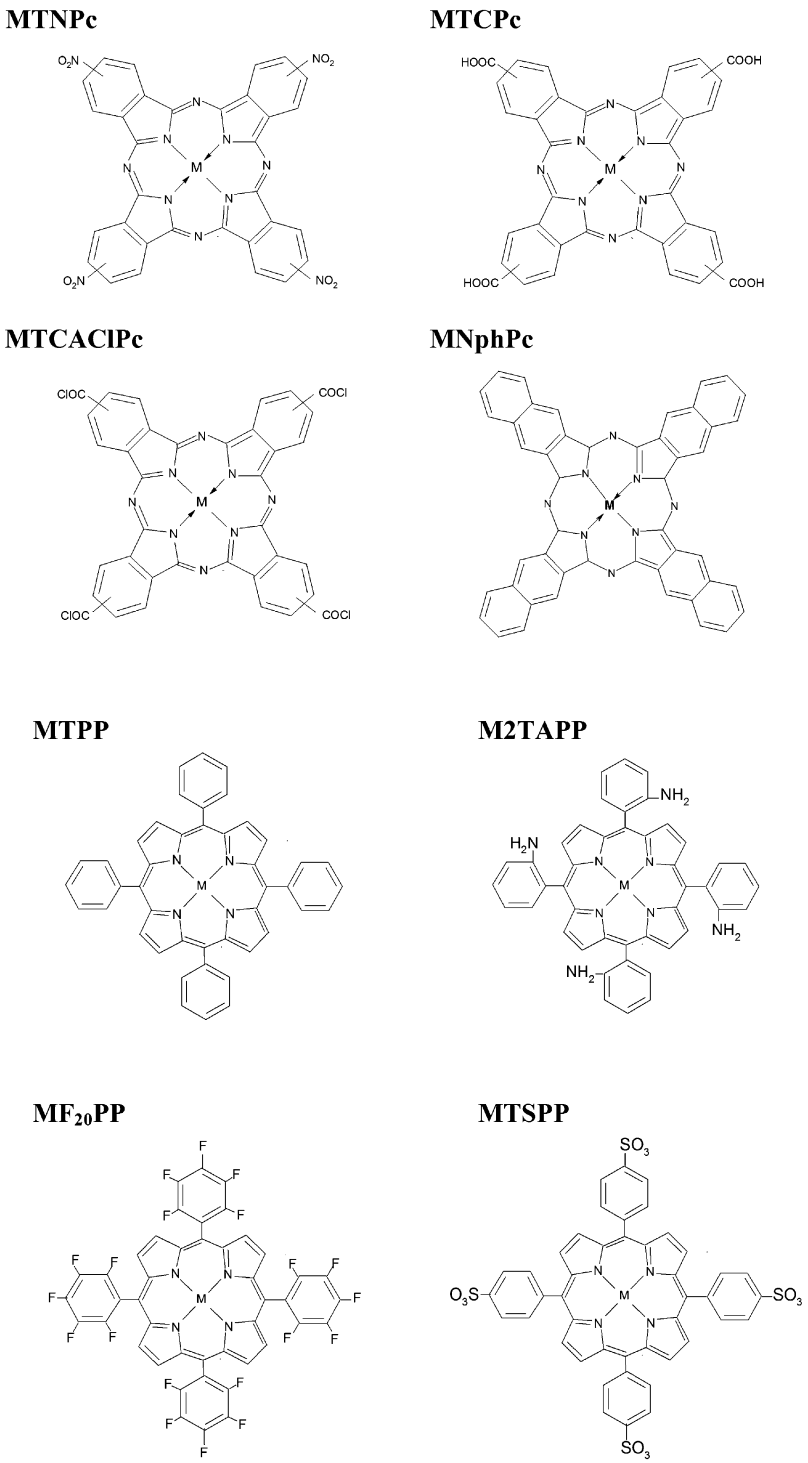

Fig. 2 Structures of metallophthalocyanines and metalloporphyrins bearing different substituents: MTNPc metallo-tetranitrophthalocyanine; MTCPc metallo-tetracarboxylphthalocyanine; MTCAClPc metallo-tetracarboxylicacidchloride phthalocyanine; MNphPc metallo-2,3-naphthalocyanine; MTPP metallo-tetraphenylporphyrin; M2TAPP metallo-2,2′,2″,2‴tetra-aminotetraphenylporphyrin; $MF_{20}PP$ metallo-pentafluorotetraphenylporphyrin; MTSPP metallo-tetrasulfotetraphenylporphyrin.

cobalt complexes including porphyrins and phthalocyanines bearing Co(II)/(I) redox potentials in the range −1.2 to −0.6 V, the correlations exhibit a maximum or have the shape of a parabola,[67] with Co-tetraaminophenylporphyin having a Co(II)/Co(I) formal potential at *ca.* −0.9 V *vs.* SCE showing the highest activity. Recently, we have investigated these correlations using adsorbed substituted metallo tetraphenylporphyrins and metallo phthalocyanines with Co as the central metal with substituents on the periphery of the N_4 ligand, using both electron-donor and electron-acceptor groups to

achieve a great variety of Co(II)/Co(I) redox potentials.[68] This illustrates the concept that the redox potential of the catalyst needs to be "tuned" in a potential range for achieving maximum activity. These findings have an impact on the design of metal complex catalysts for applications in electrocatalysis and the development of electrochemical sensors.[7]

In this article we focused on the description of some significant recent examples reported in the literature related to the electro-activation of thiols by "molecular porphyrin electrodes" and "molecular phthalocyanine electrodes". It is aimed at showing how the redox and electrocatalytic activities of the electrodes can be finely tuned in order to control the electron transfer rates.

2. Immobilization of metallo-macrocycles. Adsorption, self assembly and electropolymerization

Fig. 3 illustrates the different most common ways of attaching MN_4 macrocycles on electrode surfaces.[7] Direct electrochemistry of metal macrocycles immobilized on electrode surfaces offers a number of advantages compared to redox studies in solution, as diffusion processes involving the catalysts are eliminated. However, theoretical studies of these systems become more difficult due to the complexity of the electrode/electrolyte interface. Nevertheless, adsorption of the complexes on low area graphite or carbon materials (see Fig. 3a) has been the preferred method of most authors for fundamental and systematic studies of these systems since they provide reproducible results and the modified electrode surface can be characterized by simple techniques like cyclic voltammetry. The amount of immobilized catalyst present can be estimated and the formal potentials can be measured under the same conditions for which the catalytic activity is investigated. In a typical experiment, the adsorption of monolayers of MP or MPc is simply achieved by dipping the electrode into solutions of the complexes in different solvents for 2 to 120 min, or placing a drop of these solutions on the electrode surface for 5 to 20 min and then rinsing by ethanol or other solvent to eliminate excess of complex.

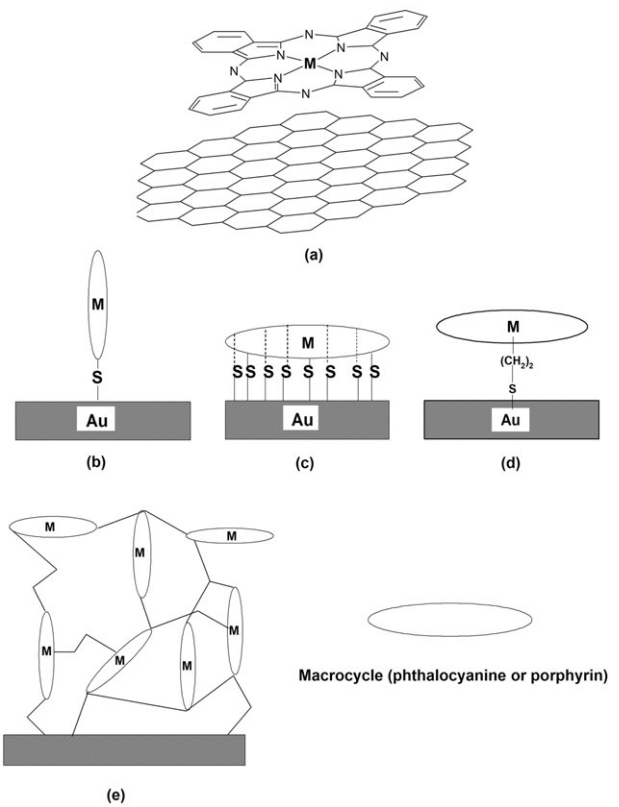

Fig. 3 Typical ways of immobilizing macrocyclic complexes on electrode surfaces: (a) by adsorption on graphite, (b) vertical and (c) octopus orientation of a thiol derivatized MPc complexes on gold to form SAMs; (d) axial ligation of MPc complex on 4-mercaptopyridine pre-formed SAM; (e) an illustration of a hypothetical polymer coating using MTAPP (adapted from ref. 118).

The use of self-assembled monolayers of thiol-derivatized phthalocyanines[56,69–86] is a convenient method for immobilizing these macrocyclic complexes on gold surfaces. Indeed, thiol derivatized macrocycle bound to a gold substrate *via* their thiol arms lead to the formation of reproducible and stable films of self-organized array of molecules, SAM. A schematic representation of these SAMs is given in Fig. 3b and c. Such a single layer of highly oriented molecules on a substrate is formed spontaneously on immersing a solid substrate into a solution containing the desired species with an appropriate functional group. Phthalocyanine-based SAMs have been formed on electrode surfaces such as platinum, mercury,[79] InSb[80] and graphite,[81] but the most common ones are those formed by reactions of thiols at gold or silver surfaces, or silanes on silica surfaces. Careful placement of thiol groups of the adsorbate can constrain the resulting molecule to a particular packing preference on the surface (see Fig. 3b and c). However, self-assembled monolayers have also been formed using amino substituted MPc complexes[73,74] on silver and gold, MPc complexes containing trichlorosilylalkyl chains on silicon or glass substrates[75] and substituted or unsubstituted MPc complexes on pre-formed SAM on gold,[82–86] Fig. 3d.

MP and MPc-containing polymers may be formed on different conductive substrates by electropolymerising a functionalized monomer directly onto a surface of an electrode or by coating the electrode with a preformed polymer. Alternatively, these complexes may be (i) incorporated into pre-formed polymers on substrates,[87–105] (ii) plasma polymerised[105–108] onto substrates or (iii) formed by the Langmuir–Blodget (LB) method.[72,109]

Electrochemical polymerisation is an elegant, attractive and easy strategy for the immobilization of metal complexes[30,110–116] on the surface of electrodes. The principle is based on the electrochemical oxidation (or reduction) of a suitably designed monomer to form a polymeric film incorporating the metal complex. The obtained polymeric films should be electronic conductors to ensure electron transfer within the matrix (and then the continuous growth of the polymers). Pyrrole-, thiophene- and aniline-based monomers have been the most commonly used materials.[114–118] Such chemically substituted monomers have many interesting features including a high flexibility in their molecular design. Additionally, such materials offer the possibility of using

either aqueous or organic solutions to carry out the electropolymerisation.

One of the first examples that involved the incorporation of metalloporphyrin and metallophthalocyanine complexes into polypyrrole films was based on the ion-exchange properties of the oxidized polymer. Tetrasulfonated substituted complexes[119–130] have been introduced into polypyrrole films as counter-ions (or "doping" ions). While several electropolymerisable pyrrole substituted metalloporphyrins have been reported in the literature, only two examples have described the electropolymerisation of pyrrole-substituted metallophthalocyanine complexes.[131,132] In the first one, the electropolymerisable pyrrole group was separated from the phthalocyanine macrocycle by an alkylene spacer. The authors reported on the formation of thick films by oxidative electropolymerisation under potentiodynamic conditions or constant potential, but no electrochemical and electrocatalytic activities were thoroughly investigated. Later on, the synthesis of a new series of pyrrole substituted phthalocyanines was reported.[133] In these, the pyrrole was separated from the phthalocyanine by a phenoxy group (namely tetrakis-4-(pyrrol-1-yl)phenoxy metal phthalocyanines).

Most studies of electropolymerised MPc have focused on the electrochemical polymerisation of MTAPc complexes.[39,110,134–142] The polymerisation process of these complexes involves the oxidation of the amino group which forms radicals that initiate condensation by attacking phenyl rings of neighbouring molecules. An illustration of a hypothetical polymer coating is given in Fig. 2e.[118] Of the MTAPc complexes (tetraaminophtahlocyanines), most studies have concentrated on the CoTAPc due to the excellent electrocatalytic behaviour of these complexes towards a variety of species. CoTAPc has been electropolymerised on glassy carbon electrode,[52,54,134,136,138,139,143–148] ITO[134,135,143,145] and highly oriented pyrolytic graphite electrode.[39] A well defined Co^{II}/Co^{I} reversible couple has been observed for poly-CoTAPc.[51,136,149]

3. Redox behavior of thiols at molecular phthalocyanine and molecular porphyrin electrodes

Fig. 4 illustrates typical cyclic voltammograms recorded on ordinary pyrolytic graphite electrode modified with pre-adsorbed layers of different cobalt phthalocyanines. All complexes exhibit a reversible pair of peaks between −0.8 and −0.2 V *vs.* SCE that is assigned to the Co^{II}/Co^{I} reversible process.[3,29,35,44,46,62] CoTAPc shows an additional pair of peaks around −0.3 V that is assigned to the substituted phthalocyanine ring.[51] These data show that, as expected, the apparent formal potential of the Co(II)/Co(I) redox process shifts to more negative values by the effect of electron donating groups (CoOEHPc, CoMeOPc, CoTNPPc and CoTAPc) since these groups increase the electron density on the metal center, making its oxidation more favourable compared to H-substituted CoPc. The opposite effect is observed for electron withdrawing groups, as the formal potential is clearly shifted to more positive values in comparison to CoPc. This is again illustrated in Fig. 5 that shows the linear correlation between the Co(II)/Co(I) formal potential and the sum of the Hammett parameters σ of the substituents on the ligand.

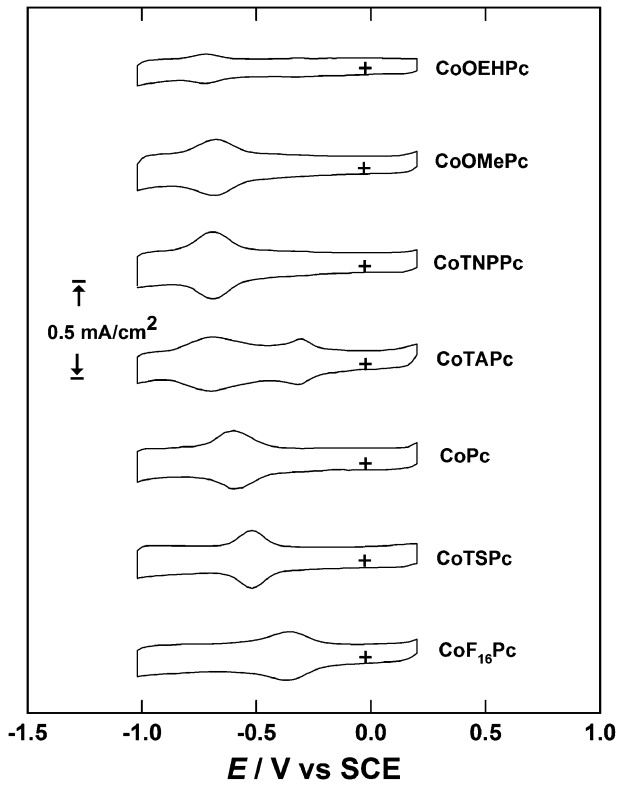

Fig. 4 Typical cyclic voltammograms in deaereated 0.2 M NaOH for an OPG electrode modified with different Co phthalocyanines. Scan rate: 0.1 V s^{-1}

Fig. 6 illustrates the typical response of a CoPc adsorbed on OPG, after adding 1 mmol L^{-1} of 2-mercaptoethanol to the electrolytic 0.1 mol L^{-1} NaOH solution. In these conditions, a large oxidation current is observed starting at −0.4 V, which is related to the electrocatalytic oxidation of 2-ME at the molecular phthalocyanine electrode. The appearance of the oxidation peak at E_{pa} = −0.2 V is concomitant with that of a reduction peak at about −1.0 V, during the reverse scan. This

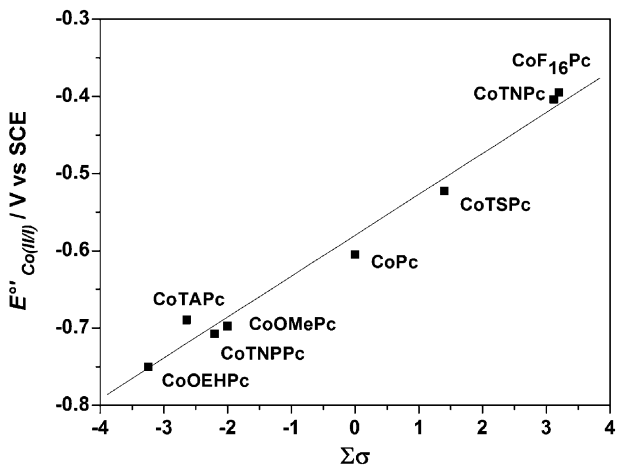

Fig. 5 Dependence of the Co(II)/(I) formal potential of the adsorbed Co phthalocyanines (data taken from Fig. 3) with the sum of the Hammett parameters of the substituent on the ligand.

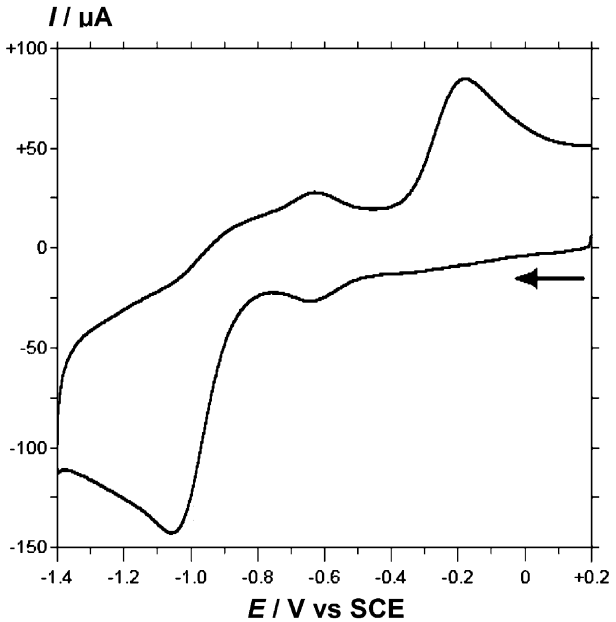

Fig. 6 Typical cyclic voltammogram of an OPG/CoPc electrode recorded in a 0.1 M NaOH deaerated solution containing 0.001 M 2-mercaptoethanol. Scan rate: 0.1 V s^{-1}.

large cathodic peak is related to the reduction of the corresponding disulfide. Indeed, if the upper limit of the anodic scan is limited to −0.45 V, the $Co^{II} \rightarrow Co^{I}$ reduction process remains unmodified, compared to the one observed without 2-ME. If the upper limit of the anodic scan is gradually increased, oxidation of 2-ME begins and the cathodic peak at −1.0 V appears and becomes larger since the reduction current linked to the disulfide reduction merges with that of the cobalt sites. It should be noted that no oxidation of 2-ME is observed at the bare electrode in the examined potential range, between −1.30 and 0 V. This clearly shows that the cobalt phthalocyanine layer not only acts as a real catalyst towards the oxidation of 2-ME but also as a catalyst for the reduction of the corresponding disulfide.

It is now well known that MPc complexes containing an electroactive central metal show good catalytic activity for the oxidation of thiols.[7,29,35] When comparing the activity of phthalocyanines of different metals for the oxidation of 2-ME, the highest activity was shown by CoPc and FePc.[150] CoPc and CoTSPc complexes were the most active ones (compared to MnPc, FePc, NiPc and CuPc) for the electrocatalytic oxidation of L-cysteine.[151]

The catalytic activity of ring substituted CoTNPc, CoTAPc, CoTBPc, CoTSPc and CoTCPc adsorbed onto glassy carbon electrode increased with the ring substituent as follows: CoTCPc > CoTBPc > CoTSPc > CoTAPc > CoTNPc. The potential for the catalytic oxidation of L-cysteine was closely related to the Co^{III}/Co^{II} couple of the CoPc species in acid media and to Co^{II}/Co^{I} couple in basic media.[46,58] The Fe^{II}/Fe^{I} couple has also been associated to the oxidation of L-cysteine promoted by FeTSPc.[46]

The study on the effect of ring substituents on the electrocatalytic behavior of MPc complexes: FeTSPc, FeTCPc, FeOMePc, $FePc(Cl)_{16}$ and FePc adsorbed on ordinary pyrolytic graphite electrode, for the oxidation of 2-mercaptoethanol,[53] showed that complexes containing electron-withdrawing groups ($-CO_2^-$, $-SO_3^-$, Cl^-) shifted the catalytic peak to more positive potentials, and the ones containing electron-donating methoxy groups to more negative potentials.[53] The catalytic activity was measured as the current observed at constant potential for the oxidation of 2-mercaptoethanol on graphite modified with different Fe phthalocyanines. The reactivity decreased as follows: FeOMePc > FePc > FeTCPc > FeTSPc > $FePc(Cl)_{16}$.[53] It was also found that the most active catalysts showed a higher reversibility for the RSH/RSSR couple.

Platinum group metal phthalocyanine monomers adsorbed on glassy carbon electrode catalyze the oxidation of L-cysteine depending on the nature of axial ligands.[59] When DMSO or cyanide were employed as axial ligands, autocatalytic behavior was observed and ring based redox processes were implicated in the catalytic process. Oxidation of L-cysteine on MPc-SAMs formed from thiol substituted MPc complexes, occurred at lower potentials compared to the potential observed for its oxidation on unmodified CoPc.[152–155] The overpotentials for oxidation of homocysteine, L-cysteine and penicillamine are slightly lower on thiol substituted FePc complexes compared to the corresponding CoPc ones,[56] however the latter was found to be less susceptible to fouling.[56]

The cyclic voltammogram of L-cysteine on CoTCAClPc attached to pre-formed 2-mercaptoethanol SAM (CoTCAClPc-2-ME-SAM) showed two well-resolved oxidation peaks. The most anodic peak was assigned to catalytic oxidation L-cysteine on 2-ME-SAM which was not coordinated to the CoTCAClPc complex,[86] while the peak at the less positive potential (0.2 V below) was assigned to the oxidation of L-cysteine on the CoCAClPc part of the SAM.[86] Of a series of MPc-4-MPy-SAM (M = Fe, Mn, Co and 4-M-Py = 4-mercaptopyridine) used for catalytic oxidation of L-cysteine, FePc-4-MPy-SAM showed better catalytic activity.[85]

From the study on the catalytic behavior of adsorbed or polymeric cobalt tetraamino phthalocyanine (poly-CoTAPc) towards the oxidation of 2-mercaptoethanol,[51] it was shown that the sensitivity and stability of poly-CoTAPc was much higher than for adsorbed monomer for 2-ME oxidation. The catalytic activity of poly-CoTAPc towards oxidation of thiols such as 2-ME, L-cysteine and reduced glutathione, was found to be similar to that of adsorbed CoTAPc (on vitreous carbon electrode) in terms of current and peak potential[54] showing that only a few external layers of the polymer are electroactive. Poly-CoTAPc was found to show catalytic activity for both the oxidation of thiols and the reduction of the corresponding disulfides.[51]

In addition to studies on adsorbed monomers, polymers and SAMs, other methods of electrode modifications for the detection of thiols have been explored. CoPc supported on poly(2-chloroaniline) acted as catalyst for the electrooxidation of 2-mercaptoethanol, reduced glutathione and hydrazine.[155] The use of CoPc composite electrode resulted in the lowering of overpotential for glutathione oxidation by 0.75 V[156] compared to the unmodified electrode. Also, MPc modified carbon paste electrodes have been employed by several authors for the analysis of thiols. Carbon paste electrodes incorporating

$OMo^{V}(OH)Pc$ catalyzed the oxidation cysteine with a considerable reduction in overpotential,[43] the oxidation of L-cysteine was mediated by $Mo^{VI}Pc$ species.[43] Carbon paste electrodes modified with CoPc also showed catalytic activity for the detection of thiocarbonyl compounds (thiourea, thioacetamide, thiobenzamide and dithiooxamide[59,157]) and the oxidation of thioglyconic acid.[59] The latter occurred *via* a two step process, which leads to the formation of the dimer of the thiol.

Only few examples have been reported in the literature on the activity of metalloporphyrin based-electrodes towards thiol oxidation.[52] They were mainly conducted with electropolymerisable porphyrins. Electrodes modified with electropolymerised aminophenyl and hydroxyphenyl cobalt porphyrins exhibit electrocatalytic activity towards the oxidation of 2-ME and L-cysteine. However, the activity of these electrodes, compared to that obtained with phthalocyanine-based ones[52] evidenced that "porphyrin electrodes" were less active than the "phthalocyanine" ones. These differences in behavior were attributed to a different electrocatalytic mechanism and/or to differences in the polymer film conductivities.

4. Trends in reactivity of macrocycles for the oxidation of thiols

The theory of electrocatalysis is still underdeveloped. In general, predictions of reactivities, with a few notable exceptions, have thus far been mainly based on correlative approaches. Along these lines, most of the work published has been focused on the electrocatalytic activity of metals for well known reactions such as hydrogen evolution or O_2 reduction. Crucial parameters that correlate with catalytic activity are heats and free energies of adsorption of reactants or intermediates that account for the interaction of the reacting molecule with the active sites located on the metal surface. In relation to the electrocatalytic activity of electrodes modified with MN_4 complexes there are no models available, but correlations can be found if the reactivity is compared *versus* some parameter that accounts for the reactivity of the active site which is the central metal.

The generally accepted mechanism for the oxidation of thiols in alkaline media involves the formation of an adduct between the metal center in the complex which acts as the active site and the thiolate. It can be written as follows:

$$RSH_{sol} + OH^- \rightleftharpoons RS^-_{sol} + H_2O \qquad \text{(step 1)}$$

$$[M(II)Pc]_{ad} + RS^-_{sol} \rightleftharpoons [R\text{-}S\cdots M(I)Pc]^-_{ad} \qquad \text{(step 2)}$$

$$[R{-}S\cdots M(I)Pc]^-_{ad} \rightarrow [M(II)Pc]_{ad} + RS^{\bullet}_{sol} + e^- \qquad \text{(step 3)}$$

$$RS^{\bullet}_{sol} + RS^{\bullet}_{sol} \rightarrow RS\text{-}SR_{sol} \qquad \text{(step 4)}$$

In this reaction scheme, step 3 is rate determining as will be discussed below. Step 4 is fast and irreversible. A crucial step is step 2, which involves a partial reduction of the metal center in the catalyst and partial oxidation of the bound thiol molecule. The redox potential can then be used as a parameter of reactivity as reduction of the metal center is involved in step 2. This is not only valid for the oxidation of thiols but also for many other reactions promoted by these MN_4 complexes[7,29,158] that can involve the formation of an adduct.

Two approaches can be used to modulate the redox potential of the complexes: (a) use of complexes with different metal centers but having the same ligand; (b) use of complexes with the same metal center but with different macrocyclic ligand.

By using approach (a) Fig. 7 compares the reactivity of two families of MPc for the oxidation of 2-ME, namely unsubstituted and tetra-sulfonated phthalocyanines.[47,49,50] The activity as log *i* (current density) at constant potential has been plotted *versus* the redox potential of the first reduction process of the catalyst (called "redox potential of the catalyst"). In these correlations, the constant potential has been chosen so currents for different catalysts can be obtained directly from Tafel plots avoiding too much extrapolation.[47,49,50,150] A linear correlation is found in both cases and the activity increases as the redox potential becomes more positive. One would expect this on thermodynamic grounds if the redox potential represents part of the driving force of the reaction (apart from the electrode potential, which in this case has been kept constant). However, activity should also increase if the affinity of the central metal for the thiol increases. What is

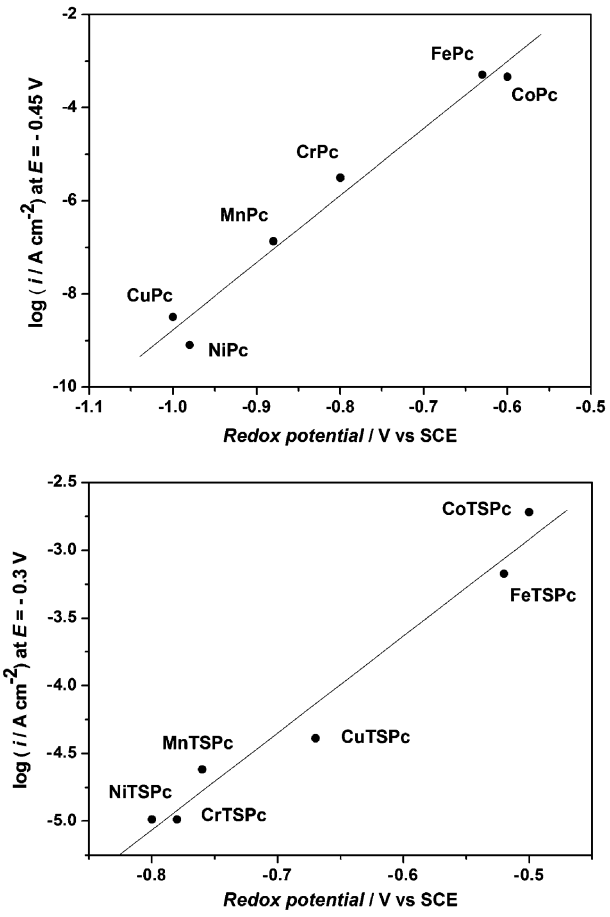

Fig. 7 Plots of log *i* (current density in A cm^{-2}) at constant potential *versus* the redox potential of the phthalocyanines and tetrasulfophthalocyanines of different metals for the oxidation of 2-mercaptoethanol in 0.2 M NaOH. Data obtained for mass transport corrected Tafel plots and adapted from Fig. 4 of ref. 47 and Fig. 2 of ref. 49.

interesting in the data shown in Fig. 7 is that for example the effect of the ligand depends on the nature of the central metal. When comparing CrPc with CrTSPc, CrPc is more active than CrTSPc. In contrast, CuTSPc is more active than CuPc but in both cases no deviations are observed from the linear correlation, so the redox potential is a good reactivity index for these complexes no matter what central metal or what ligand is used. Another interesting feature in the correlations of Fig. 7 is that the slopes for both families of phthalocyanines are different. For unsubstituted MPcs, the slope is 0.070 V decade^{-1} whereas for MTSPcs is 0.14 V decade^{-1}. On the other hand, Tafel slopes obtained from plots of log *i versus* potential for all catalysts included in Fig. 7 are less than 0.12 V decade^{-1},[49,150] and depend on the particular catalyst. As seen from the data in Tables 1 and 2 the slopes tend to be lower for the most active catalyst, so the symmetry factor β varies between 0.28 and 0.65.

Similar Tafel slopes are also observed for the oxidation of other thiols like L-cysteine catalyzed by several metallophthalocyanines,[159] the oxidation of mercaptoacetate[68] and aminoethanethiol.[62] These results have been used to justify that the transfer of one electron in step 3 is rate controlling in alkaline media.

The linear dependence of log *i* on redox potential in Fig. 7 seems to indicate that the free energy of adsorption of the thiol on the active sites is proportional to the redox potential of the catalyst since if this is true the slope would be $(1 - \beta')\Delta G_{ads}$[160] where ΔG_{ads} would account for the thermodynamics of step 2. Note that $(1 - \beta')$ is a Brønsted coeficient acting on the *rds* barrier height resulting from changing reactant adsorption before the *rds* barrier. β' is not necessarily equal to the transfer coefficient β, linked to the rate determining step 3, which results from changes in the *rds* barrier height by the effect of the potential on the Fermi level of the electrode, *i.e.* on the electron products of the *rds*. This is generally observed for correlations of this type when comparing the electrocatalytic activity of metals.[160–169] Similar correlations to those in Fig. 7 are found for the oxidation of L-cysteine on MPcs and MTSPcs with similar slopes,[47,49,50] so these correlations seem to be independent of the nature of the thiol. It must be pointed out however that only Mn, Fe and Co and probably Cr exhibit redox processes located on the metal, namely the M(II)/M(I) process. For Ni and Cu the redox potential plotted in Fig. 7 involves the ligand. It must also be pointed out that when different central metals are compared, different frontier orbitals in the metal could be involved for each particular case, when adsorption of RS^- takes place. For example, for the central metals Fe and Co, which have a frontier orbital with more *d* character[50,170,171] one would expect a stronger interaction of the metal with the thiol than, for example, Cu. There is experimental evidence using electron tunneling microscopy[170,172] that supports the theoretical calculations which suggest that the frontier orbitals in CoPc have much more metal character than those in CuPc. The tunneling microscopy images indicate that CoPc adsorbed on gold shows the highest point in the molecular image and located on the metal. In contrast, under similar conditions with CuPc, the metal center appears as a hole.[172]

Table 1 Tafel slopes for the oxidation of 2-mercaptoethanol on different M-Pcs at 25 °C, pH = 12.8

Catalyst	Slope in V decade^{-1}	RT/βF	β
NiPc	0.150	2.54 RT/F	0.39
CuPc	0.136	2.30 RT/F	0.43
MnPc	0.127	2.15 RT/F	0.46
CrPc	0.099	1.68 RT/F	0.60
CoPc	0.127	2.15 RT/F	0.46
FePc	0.113	1.91 RT/F	0.52

Table 2 Tafel slopes for the oxidation of 2-mercaptoethanol on different M-TSPcs at 25 °C, pH = 10.1 (taken from ref. 150)

Catalyst	Slope in V decade^{-1}	RT/βF	β
CrTSPc	0.167	2.83 RT/F	0.35
NiTSPc	0.120	2.03 RT/F	0.49
MnTSPc	0.114	1.93 RT/F	0.52
CuTSPc	0.096	1.62 RT/F	0.62
FeTSPc	0.082	1.39 RT/F	0.72
CoTSPc	0.093	1.58 RT/F	0.37

Since the redox potential of the catalyst seems to be a good reactivity index for the catalytic activity of these complexes it is interesting to compare the activity of complexes using approach (b), *i.e.* having the same metal center but with ligands having different substituents (electron-withdrawing or electron-donating groups), in order to modulate the redox potential. Fig. 8 compares the catalytic activity of different cobalt phthalocyanines *versus* the Co(II)/(I) formal potential for the oxidation of 2-aminoethane thiol for two electrode potentials.[62] In contrast to what is observed for phthalocyanines of different metals, the activity decreases as the formal potential of the catalyst becomes more positive and the slope is −0.181 V decade^{-1} or −3 RT/F at E = −0.35 and −0.273 V or −4.6 RT/F at E = 0.20 V. Similar results are observed for the oxidation of 2-mercaptoethanol catalyzed by iron phthalocyanines[53] and the slopes are −0.205 V decade^{-1} or −3.47 RT/F for E = −0.30 V and −0.370 V decade^{-1} (−6.27 RT/F) for E = −0.25 V. This shows that the slopes are sensitive to the

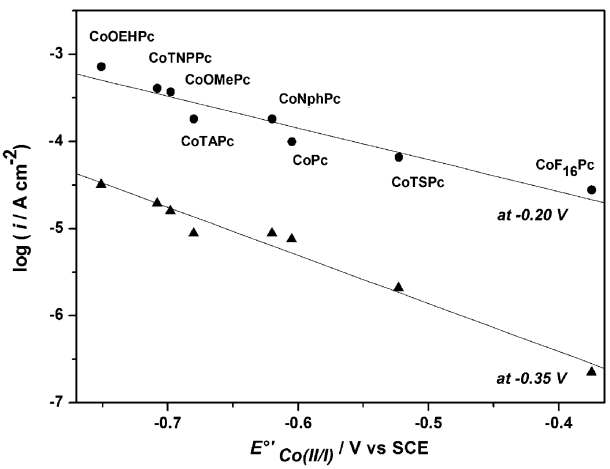

Fig. 8 Plot of log *i* (current density in A cm^{-2}) at constant potential *versus* the Co(II)/(I) formal potential of different Co phthalocyanines confined on an OPG electrode for the oxidation of 2-aminoethanethiol in 0.2 M NaOH. Data obtained for mass transport corrected Tafel plots at −0.20 and at −0.35 V *vs.* SCE taken from ref. 62.

Table 3 Variation of the slope (in V decade^{-1}) of plots of log *i versus* $E^{o\prime}$ for the oxidation of several thiols in basic media (pH = 13) catalyzed by Co phthalocyanines confined on graphite

Electrode potential/V *vs.* SCE	2-Aminoethanethiol	2-Mercaptosulfonic acid	L-Cysteine	2-Mercaptoethanol
−0.450				−0.234
−0.400				−0.267
−0.350	−0.181			−0.283
−0.300	−0.220			−0.273
−0.250	−0.261			
−0.200	−0.273	−0.225	−0.220	−0.300
−0.150		−0.250	−0.218	
−0.100		−0.257	−0.224	
−0.050		−0.240	−0.220	

potential chosen for comparison and tend to increase as the potential becomes more positive. In general, the slopes of the plots of log *i versus* redox potential are also negative and potential-dependent for the oxidation of several thiols, as illustrated in Table 3.

In order to include a wider variety of Co(II)/(I) redox potentials, cobalt porphyrins together with cobalt phthalocyanines and vitamin B_{12} (aquocobalamine) were investigated and the results are included in Fig. 9 for the oxidation of 2-mercaptoethanol. In this case a volcano-shaped curve is obtained, with a region where activity increases with the Co(II)/(I) formal potential and another region where the activity decreases. The slope of the ascending portion of the volcano is 0.110 V decade^{-1} or 1.86 *RT*/F and the declining portion has a slope of −0.245 V decade^{-1} or −4.15 *RT*/F. We have obtained similar results to those illustrated in Fig. 9 for the oxidation of 2-mercaptoethanol when glassy carbon is used instead of pyrolytic graphite.[67] The slope of the ascending portion of the volcano in that case was 0.125 V decade^{-1} or 2.12 *RT*/F and −0.218 V decade^{-1} or −3.69 *RT*/F for the declining portion. This shows that the correlations of activity *versus* the formal potential of the catalyst do not depend on the substrate used for confining the complexes.

A similar correlation is observed for the oxidation of 2-mercaptoacetate and the data are illustrated in Fig. 10. The volcano plot of Fig. 10 includes Co porphyrins, Co phthalocyanines and cyanocobalamin (vitamin B_{12}). As observed for the oxidation of 2-ME a linear region of positive slope (0.112 V decade^{-1} or 1.90 *RT*/F) is observed and then a region where activity decreases with the formal potential of the catalysts with a slope equal to −0.171 V decade^{-1} (−2.90 *RT*/F). It has been established empirically that a volcano-shape curve is obtained when the activity of the catalyst (logarithm of current density) for a given reaction is plotted *versus* a parameter related to the ability of the catalyst to form chemical bonds with reactants, reaction intermediates or products.[165–169,173–178] These relations are interesting from the fundamental point of view as they point to important aspects of the reaction and they serve as guidelines in the search of new catalysts.

For these correlations to be valid it is important that the following requirements are met, namely:

(i) The overall reaction must be the same on all different catalysts under study, *i.e.* the rate determining step must be the same in each case, and the reaction path, at least as far as the rate determining step, must also be the same.

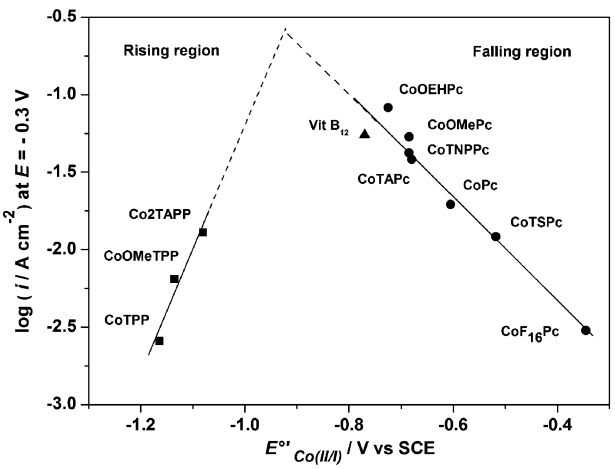

Fig. 9 Plots of log *i* (current density in A cm^{-2}) *versus* the Co(II)/(I) formal potential of different cobalt N_4 macrocycles confined on OPG for the oxidation of 2-mercaptoethanol in 0.1 M NaOH. Data obtained for mass transport corrected Tafel plots at E = −0.30 V *vs.* SCE.

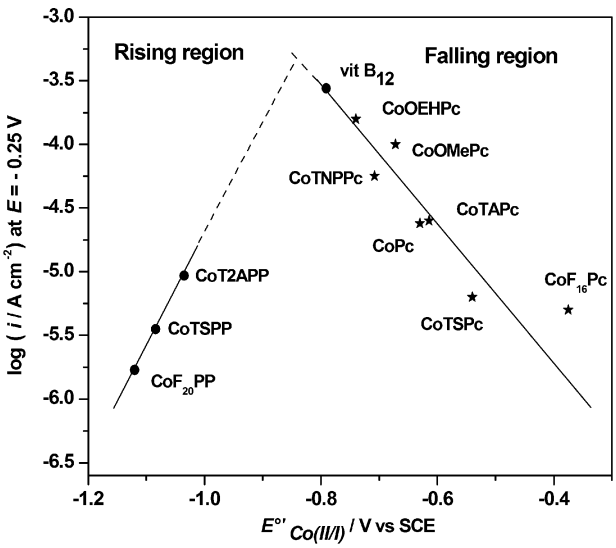

Fig. 10 Plots of log *i* (current density in A cm^{-2}) *versus* the Co(II)/(I) formal for the oxidation of 2-mercaptoacetate in 0.1 M NaOH, on OPG modified with different cobalt N_4 macrocycles. Data obtained from Tafel plots at E = −0.250 V *vs.* SCE, from ref. 68 (currents in A cm^{-2} corrected for mass transport).

(ii) The process must be compared over a series of catalysts under identical conditions, so the rates are only affected by interactions between reaction intermediates, the solvent and the electrode surface.

These conditions are met for the data reported in this work. Heats of adsorptions of the molecules on different catalysts or bond strengths between active site and the adsorbed molecule are generally used in volcano plots.[160] In the case of the data in Fig. 6–10, the redox potential is used since heats and free energies of adsorption of thiols on the different metal N_4-macrocycles are not available in the literature. However the formal potential is related to the reactivity of the metal center towards the thiol through adduct formation and to the thermodynamics of this process (step 2). Thus, the data in the volcano plots can be explained according the above written mechanism (the thiolate is used since all data in Fig. 6–9 were obtained in alkaline media (pH in the range 10 to 13).

Using a Langmuir isotherm for the adsorbed RS^-, its coverage θ can be written as follow:

$$\theta/(1-\theta) = a\mathrm{RS}^-_{\mathrm{sol}} \exp(-\Delta G_{\mathrm{RS}^-}/RT) \qquad (1)$$

where ΔG_{RS^-} is the free energy of adsorption of RS^- (as [R-S$\cdots$M(I)Pc] in step 2 relative to $a\mathrm{RS}^-_{\mathrm{sol}}$, the solution activity of the thiolate. Solving for θ one obtains:

$$\theta = a\mathrm{RS}^-_{\mathrm{sol}} \exp(-\Delta G_{\mathrm{RS}^-}/RT)/ \\ [1 + a\mathrm{RS}^-_{\mathrm{sol}} \exp(-\Delta G_{\mathrm{RS}^-}/RT)] \qquad (2)$$

$-\Delta G_{\mathrm{RS}^-}$ could depend on electrode potential since the process involves a charged species and could also depend on coverage. On may assume that the electrochemical *rds* has a rate constant of $k = C\exp(+\beta EF/RT)$ at $\theta = (1-\theta) = 0.5$ where E is the potential on some nominal scale and C is a constant. Assuming that the barrier height is changed by $+(1-\beta')\Delta G_{\mathrm{RS}^-}$ in the presence of adsorption keeping in mind that adsorption acts on the initial state (step 2) whereas E acts on the final state (step 3). As seen from the bottom of the energy well for $\mathrm{RS}_{(\mathrm{ads})}{}^-$, the barrier height changes by $-\beta'\Delta G_{\mathrm{RS}^-}$ in the presence of adsorption, compared with its standard state value at $\theta = 0.5$. The rate of the *rds* is therefore:

$$v = \theta C \exp(+\beta'\Delta G_{\mathrm{RS}^-}/RT) \exp(+\beta EF/RT) \qquad (3)$$

$$v = a\mathrm{RS}^-_{\mathrm{sol}} C \exp(-(1-\beta')\Delta G_{\mathrm{RS}^-}/RT) \\ \times \exp(+\beta EF/RT)/[1 + a\mathrm{RS}^-_{\mathrm{sol}} \exp(-\Delta G_{\mathrm{RS}^-}/RT)] \qquad (4)$$

At small θ, and $a\mathrm{RS}^-_{\mathrm{sol}} \exp(-\Delta G_{\mathrm{RS}^-}/RT) \ll 1$, this corresponds to the rising side of the volcano and the rate is:

$$v = a\mathrm{RS}^-_{\mathrm{sol}} C \exp(-(1-\beta')\Delta G_{\mathrm{RS}^-}/RT) \\ \times \exp(+\beta EF/RT) \qquad (5)$$

For the falling side of the volcano θ is high and $a\mathrm{RS}^-_{\mathrm{sol}} \exp(-\beta'\Delta G_{\mathrm{RS}^-}/RT) \gg 1$. The rate is then:

$$v = C \exp(+\beta'\Delta G_{\mathrm{RS}^-}/RT) \exp(+\beta EF/RT) \qquad (6)$$

Under high coverage conditions the rate becomes zero order in RS^-.

Table 4 Tafel slopes for the oxidation of 2-mercaptoacetate for catalysts on the rising side of the volcano plot of Fig. 10

Catalyst	Tafel slope	Tafel slope
$CoF_{20}PP$	0.092	1.56 RT/F
CoTSPP	0.103	1.74 RT/F
CoT2APP	0.093	1.58 RT/F

From this simplified analysis, catalysts on the rising and falling side of the volcano should have the same Tafel slope, provided that ΔG_{RS^-} does not depend on the potential. Since the reaction involves charged species ΔG_{RS^-} could be proportional to $-\gamma FE$. The rate of the reaction for the rising side of the volcano becomes:

$$v = a\mathrm{RS}^-_{\mathrm{sol}}\, C \exp(+[\beta + \gamma(1-\beta')]\, EF/RT) \qquad (7)$$

So the Tafel slope for the rising side of the volcano should be $RT/ + [\beta + \gamma(1-\beta')]$ F.

Using the same reasoning, for the falling side of the volcano the rate is:

$$v = C \exp(+(\beta - \gamma\beta')EF/RT) \qquad (8)$$

In this case, the Tafel slope for the falling side of the volcano should be $RT/\beta - \gamma\beta')$F.

On the rising side of the volcano plot of Fig. 10, the Tafel slopes are 0.093 V decade^{-1} for $CoF_{20}PP$, 0.103 V decade^{-1} for CoTsPP and 0.093 V decade^{-1} for CoT2APP (see Table 4) suggesting that γ could be different from 0. However, if $\gamma = 0$, the variation in the Tafel slopes could be attributed to changes in β. The same could be true for catalysts on the falling side of the volcano (see Table 5).

Concerning the correlations between log i and formal potential, from the slopes, the plots show (Fig. 7) $(1-\beta') = 0.84$ and 0.4 for M-Pcs and M-TSPcs (all rising sides); (Fig. 8) 0.28 V ($E = -0.30$ V) and 0.15 ($E = -0.250$ V) for Fe-Pcs (falling side); (Fig. 9) 0.42 (rising side) and 0.71 (falling side); (Fig. 10) +0.54 and 0.66 (rising and falling sides, respectively). Again, this simple treatment predicts that β' should have the same value for both branches, but Fig. 8 and 9 show this not to be the case. However, the rising branch (weak adsorption, positive ΔG, low θ) may have very differently shaped energy wells than those for the falling branch (strong adsorption, negative ΔG, high θ), so the change in β' with coverage may not be surprising. The different rising branches show a variation of $(1-\beta')$ from 0.84 to 0.4, whereas the three falling branches studied in Fig. 8, 9 and 10 have $(1-\beta') = 0.20$

Table 5 Tafel slopes for the oxidation of 2-mercaptoacetate for catalysts on the falling side of the volcano plot of Fig. 10

Catalyst	Tafel slope V decade^{-1}	Tafel slope
Vitamin B_{12}	0.091	1.54 RT/F
CoOEHPc	0.079	1.34 RT/F
CoTNPPc	0.077	1.31 RT/F
CoOMePc	0.078	1.32 RT/F
CoPc	0.094	1.59 RT/F
CoTSPc	0.075	1.27 RT/F
$CoF_{16}Pc$	0.085	1.44 RT/F
CoTAPc	0.095	1.61 RT/F

and 0.71 over a very wide range. In all cases, the rising branch of the volcanoes show slopes almost one-half of those corresponding to the falling branch for Fig. 9 and 10 and for the volcano reported in the literature.[67]

It can be concluded that, on one hand, β seems to depend on the nature of the catalyst which indicates that the shape of the energy wells might vary to some degree for each catalyst (as seen for the variation of Tafel slopes). Variations in the slopes on both sides of the volcanos or incomplete volcanos might also reflect changes in the shape of energy wells with adsorption. So eqns (3) and (4) explain the volcano curves in Fig. 9 and 10. The ascending portion of the volcano corresponds to low coverages and a maximum activity should be achieved at $\theta = 0.5$. The slopes observed experimentally are close but less than 2 RT/F and seem to indicate that the formal potential of the catalyst is directly proportional to $+\Delta G_{RS^-}$.

According to the mechanism proposed for alkaline media, the equilibrium constant of step 2 affects the rate of the reaction in the following way: step 2 is favored by redox potentials which are gradually more positive and this explains the ascending portion of the volcano. This would be equivalent to gradually decreasing $+\Delta G_{ad}$.[160–169,171–176] So increasing the formal potential increases the reactivity of the metal centers towards the thiol (formation of the adduct in step 2 becomes more spontaneous). However, increasing the formal potential of the catalyst beyond a certain value becomes detrimental since this will favor the formation of the adduct to a point where it will be occupying most of the Co active sites, preventing the interaction of new coming thiol molecules on these sites. This is true because the decomposition of the adduct in step 3 is rate controlling so if the formation of the adduct is too favourable, it will accumulate on the surface ($\theta \sim 1$). The maximum activity should be achieved when $\Delta G_{ad} = 0$[160] and $\theta = 0.5$. Then currents decrease for values of $\Delta G_{ad} < 0$ which correspond to the high coverage region ($\theta \sim 1$). An explanation is still needed for the slopes near -4 RT/F in the declining portion of the volcano. They might reflect a different shape of the energy well for high coverages which will affect the values of β'.

The above analysis offers a tentative explanation of the difference between the Tafel slopes and the Brønsted slopes at high and low coverage, but a much more satisfactory explanation is as follows: this time, we assume the reactant R-S$^-$ and product RS$^\bullet$ of the *rds* are both adsorbed:

$$[\text{R-S}^- \cdots \text{M(I)Pc}]^-_{ad} \rightarrow [\ \text{RS}^\bullet \cdots \text{M(II)Pc}]_{ad} + e^- \quad \text{(step 5)}$$

For simplicity, from now on we refer to the adsorbed thiolate anion as RS$^-{}_{ads}$ and to the adsorbed thiyl radical as RS$^\bullet{}_{ads}$. θ_1 and θ_2 are the coverages of RS$^-_{ads}$ and RS$^\bullet{}_{ads}$, respectively, whose Brønsted coefficients are β_1 and β_2, and whose free energies of adsorption are ΔG_1 and ΔG_2. We use the convention that the height of the free energy barrier for activation energy barrier (as seen from outside of the system) changes by $+\beta_2\Delta G_2$ for an adsorbed product ($+\Delta G_2$), and $+(1-\beta_1)\Delta G_1$ for an adsorbed reactant ($+\Delta G_1$). As seen by the adsorbed reactant in its energy well, the free energy barrier height changes by $-\beta_1\Delta G_1 + \beta_2\Delta G_2$. The rate of the *rds* is:

$$v = \theta_1(2k_1)\exp(+\beta_1\Delta G_1/RT)\exp(-\beta_2\Delta G_2/RT) = \theta_1 x \quad (9)$$

where k_1 is the rate constant at constant reference potential when ΔG_1 and ΔG_2 are zero, *i.e.*, when θ_1 is in its standard state equal to 0.5 (normalized by the coefficient 2). k_1 varies with potential according to the Tafel equation. We assume a Langmuir isotherm for RS$^-_{ads}$ so that $\theta_1/(1-\theta_1-\theta_2) =$ aR-S$^-_{sol}$exp $-\Delta G_1/RT$, where aR-S$^-_{sol}$ is the solution activity of RS$^-$, *i.e.*, $\theta_1 =$ aR-S$^-_{sol}(1-\theta_2)$(exp $-\Delta G_1/RT$)/(1+ aR-S$^-_{sol}$ exp $-\Delta G_1/RT$). We further assume that the RS$^\bullet{}_{ads}$ desorption step is irreversible, so the back reaction is ignored. So we have the possible steps:

Rapid desorption:

$$\text{RS}^\bullet_{ads} \rightarrow \text{RS}^\bullet_{sol}, \quad \text{(step 6)}$$

followed by $2\text{RS}^\bullet{}_{sol} \rightarrow \text{RSSR}_{sol}$ described before as step 4 or surface recombination:

$$2\text{RS}^\bullet_{ads} \rightarrow \text{RSSR}_{sol} \quad \text{(step 7)}$$

The rates of steps 6 and 7 are, respectively:

$$\theta_2(2k_2)\exp(+\beta_3\Delta G_2/RT) = \theta_2 y \quad (10)$$

and

$$\theta_2^2(4k_3)\exp(+2\beta_3\Delta G_2/RT) = \theta_2^2 z \quad (11)$$

where k_2, k_3 are potential-independent rate constants for the desorption and surface recombination processes, respectively. $+\beta_3$ is the Brønsted coefficient for the recombination process. The three Brønsted coefficients may or may not be equal, and may or may not be equal to the electrochemical symmetry factor β. Because medium-coverage conditions exist in a very limited free energy of adsorption range, we need only consider low- and high-coverage cases for RS$^-_{ads}$. For case of step 6 (the least probable of the two reactions following the *rds* at low coverage of RS$^-_{ads}$, $\theta_1 \approx$ aR-S$^-_{sol}(1-\theta_2)$exp$(-\Delta G_1/RT)$. Using the steady-state hypothesis, and equating the rates of (9) and (10):

$$\begin{aligned} \text{aR-S}^-_{sol}(1-\theta_2)\exp(-\Delta G_1/RT\ ) = \theta_2 y,\ \textit{i.e.},\ (1-\theta_2) \\ = y/[\ \text{aR} - \text{S}^-_{sol}\text{xexp}(-\Delta G_1/RT) + y] \end{aligned} \quad (12)$$

From the *rds* assumption, the rate aR-S$^-_{sol}$xexp$(-\Delta G_1/RT) < y$, so $(1-\theta_2) \approx 1$. Hence, $\theta_1 \approx$ aR-S$^-_{sol}$exp$(-\Delta G_1/RT)$ and (11) becomes:

$$\begin{aligned} v = \text{aR-S}^-_{sol}(2k_1)\exp(-(1-\beta_1)\Delta G_1/RT) \\ \times \exp(-\beta_2\Delta G_2/RT) \quad \text{(low coverage)} \end{aligned} \quad (13)$$

For case of step 6 (rapid desorption) at high coverage of RS$^-_{ads}$, $\theta_1 \approx (1-\theta_2)$, so $(1-\theta_2) = \theta_2 y$, *i.e.*, $(1-\theta_2) = y/(y+x)$ So (9) becomes, with $y \gg x$,

$$v = (2k_1)\exp(+\beta_1\Delta G_1/RT)\exp(-\beta_2\Delta G_2/RT) \quad \text{(high coverage)} \quad (14)$$

If we now perform the same operations using the more probable of surface recombination assumptions (step 7) , at low coverage of RS$^-_{ads}$, again $\theta_1 =$ aR-S$^-_{sol}(1-\theta_2)$exp$(-\Delta G_1/RT)$, while at high coverage $\theta_1 = (1-\theta_2)$. In both cases, $\theta_1 x = \theta_2{}^2 z$. The resulting quadratics have approximate solutions for θ_2 equal to $(q)^{0.5}(1 + q/8) - q/2$, where q is aR-S$^-_{sol}$ (x/z)exp$(-\Delta G_1/RT)$ (low coverage) or (x/z) (high coverage).

Because of the *rds* assumption, q is a relatively small number, and in many cases the linear term in θ_2 in the quadratic can be ignored, so $\theta_2 \approx q^{0.5}$, which may be somewhere in the range from about 0.6 to smaller values. Hence $(1-\theta_2)$ is about 0.4 to unity, which is a small range on a log rate scale. The rates of the *rds* for low and high coverage are therefore approximately: $v = \mathrm{aR\text{-}S^-_{sol}}(2k_1)\exp(-(1-\beta_1)\,\Delta G_1/RT)\exp(-\beta_2\Delta G_2/RT)$ (low coverage) and $v = (2k_1)\exp(+\beta_1\Delta G_1/RT)\exp(-\beta_2\Delta G_2/RT)$ (high coverage) which are identical with (13) and (14), within the limits of the approximation. Thus, no matter what is the desorption process, the rate relationships are the same. They follow $\exp[-(1-\beta_1)\,\Delta G_1/RT - \beta_2\Delta G_2/RT]$ at low coverage of $\mathrm{RS^-_{ads}}$, and $\exp(+\beta_1\Delta G_1/RT - \beta_2\Delta G_2/RT)$ at high coverage of this anion. We can only speculate about the values of $(+\beta_1\Delta G_1/RT - \beta_2\Delta G_2/RT)$, but it is not unreasonable to suppose that both β_1 and β_2 may be fairly close to 0.5, and that ΔG_1 for the charged species $\mathrm{RS^-_{ads}}$ may be fairly similar to ΔG_2 for the uncharged radical $\mathrm{RS^{\bullet}_{ads}}$. Thus, the overall Brønsted coefficient for any low coverage case for $\mathrm{RS_{ads}}^-$ may be close to unity, while that for the high coverage case may be $\approx\beta_1 - \beta_2$, *i.e.*, a fraction of unity. The Brønsted slope at low coverage may then be about RT/F, while the corresponding slope at high coverage may be several times RT/F. This is an alternative explanation for the asymmetry of the parabolic correlations of log *i versus* $E^{o\prime}$ in Fig. 9 and 10.

5. Conclusions

The data in Fig. 9 and 10 clearly shows that the search for better catalysts for this reaction points to those N_4-macrocyclic complexes with formal potentials corresponding to an optimum situation for the interaction of the thiol with the active sites. For the oxidation of 2-mercaptoethanol the highest activity is observed for $E^{o\prime} = -0.93$ V for catalysts adsorbed on graphite and at $E^{o\prime} = -0.95$ V for catalysts adsorbed on glassy carbon[67] whereas for 2-mercaptoacetate oxidation maximum activity is achieved for $E^{o\prime} = -0.85$ V. So the optimum formal potential depends on the nature of the thiol and is linked to the thermodynamics of adduct formation.

N_4-macrocycles like metalloporphyrins and metallophthalocyanines are active catalysts for the electrooxidation of a great variety of thiols. Catalytic surfaces containing these complexes can be obtained by simple adsorption on graphite surfaces. However, more stable electrodes can be achieved by using electropolymerised complexes which show similar activity than their monomer counterparts. Modified electrodes can be obtained on Au and Ag surfaces by using self-assembled monolayers of thiols that can act as anchors of macrocyclic complexes or by using complexes with thiol functionalities located on the periphery of the ligand, also serving as anchors. Electrodes modified in this fashion show catalytic activity for the oxidation of thiols so essentially, the activity of the metallophthalocyanines and metalloporphyrins is almost independent of the method employed for modification and seems to be independent of the orientation of the macrocyclic molecule on the electrode.

Fundamental studies carried out at monolayer levels of these complexes on graphite and carbon surfaces have demonstrated that the redox potential of the complex plays a very important role in the catalytic process. When a great variety of Co complexes are used, showing Co(II)/(I) formal potentials in a wide window of potentials, plots of log *i versus* $E^{o\prime}$ have the shape of an unsymmetric parabola or volcano. This indicates that the $E^{o\prime}$ formal potential of the catalyst is an indication of the reactivity of the central metal towards the thiol molecule. The parabolic curves suggest that intermediate values of $E^{o\prime}$ are optimum for achieving maximum activity, probably corresponding to surface coverages of an Co-thiol adduct equal to 0.5 and to free energies of adsorption equal to zero. All these results indicate that the catalytic activity of metallo macrocycles for the oxidation of thiols can be "tuned" by manipulating the $E^{o\prime}$ formal potential using the proper groups on the ligand. "Tuning" the redox potential can be achieved by knowing the Hammett parameters of substituents that can be located on the ligand for families bearing the same ligand. These results are probably valid for the different methods of modification of the electrode and point out to the right direction in designing better catalysts for the oxidation of thiols and other electrochemical reactions.

Acknowledgements

This work was funded by Fondecyt Project 1060030. Financial support from ECOS-Sud (France)/Conicyt (Chile) program C03E02 and Conicyt/CNRS exchange program 206/2007 for travel expenses is acknowledged. T.N. thanks National Research Foundation (NRF, GUN 2053657) for support.

References

1 A. B. P. Lever, M. R. Hempstead, C. C. Leznoff, W. Liu, M. Melnik, W. A. Nevin and P. Seymour, *Pure Appl. Chem.*, 1986, **58**, 1467.
2 E. Orti and J. L. Brédas, *J. Am. Chem. Soc.*, 1992, **114**, 8669.
3 C. C. Leznoff and A. B. P. Lever, in *Phthalocyanines Properties and Applications*, VCH Publishers Inc., New York, 1989, vol. 1–4.
4 D. Dolphin, in *The Porphyrins*, Academic Press, New York, 1978, vols. I–VII.
5 B. D. Berezin, in *Coordination Compounds of Porphyrins and Phthalocyanines*, John Wiley & Sons Ltd., New York, 1981.
6 K. M. Kadish and K. M. Smith, in *The Porphyrin Handbook*, ed. R. Guilard, Academic Press, New York, 2003, vol. 1–20.
7 *N-4 Macrocyclic Metal Complexes*, ed. J. H. Zagal, F. Bedioui and J. P. Dodelet, Springer, New York, 2006.
8 C. W. Tang, *Appl. Phys. Lett.*, 1986, **48**, 183.
9 *Phthalocyanine Research and Applications*, ed. A. L. Thomas, CRC Press, Boca Raton, FL, 1990.
10 *Molecular Semiconductors*, ed. J. Simon and J. J. Andre, Springer, Berlin, 1986.
11 *Phthalocyanine Materials: Synthesis, Structure and Function*, ed. N. B. McKeown, Cambridge University Press, Cambridge, 1998.
12 M. Kato, Y. Nishioka, K. Kaifu, K. Kawamura and S. Ohno, *Appl. Phys. Lett.*, 1985, **46**, 196.
13 R. A. Collins and K. A. Mohammed, *J. Phys. D: Appl. Phys.*, 1988, **21**, 154.
14 F. Bedioui, S. Gutierrez-Granados and C. Bied-Charreton, *Recent Res. Devel. Electrochem.*, 1999, **2**, 91.
15 R. O. Loutfy, A.-M. Hor, C.-K. Hsiao, G. Baranyi and P. Kazmaier, *Pure Appl. Chem.*, 1988, **60**, 1047.
16 T. A. Temofonte and K. F. Schoch, *J. Appl. Phys.*, 1989, **65**, 1350.
17 N. Toshima and T. Tominaga, *Bull. Chem. Soc. Jpn.*, 1996, **69**, 2111.
18 A. H. Ghosh, D. L. Morel, T. Feng, R. F. Shaw and C. A. Rowe, *J. Appl. Phys.*, 1974, **45**, 230.
19 B. W. Flynn, A. E. Owen and J. Mavor, *J. Phys. C: Solid State Phys.*, 1977, **10**, 4051.

20 J. Simon and C. Sirlin, *Pure Appl. Chem.*, 1989, **61**, 1625.
21 T. J. Marks, *Angew. Chem., Int. Ed. Engl.*, 1990, **29**, 857.
22 M. K. Casstevens, M. Samoc, J. Pfleger and P. N. Prasad, *J. Chem. Phys.*, 1990, **92**, 2019.
23 S. Palacin, P. Lesieur, I. Stefanelli and A. Barraud, *Thin Solid Films*, 1988, **159**, 83.
24 *Katalyse und Phthalocyaninen*, ed. H. Kropf, F. Steinbach, Georg Theme Verlag, Stuttgart, 1973.
25 B. Basu, S. Satapathy and A. K. Bathnagar, *Catal. Rev. Sci. Eng.*, 1993, **35**, 571.
26 T. Buck, H. Bohlen, D. Wöhrle, G. Schulz-Ekloff and A. Andreev, *J. Mol. Catal.*, 1993, **80**, 253.
27 F. V. Iliev, I. A. Ileva, D. L. Dimitrov and D. Lyubomin, *Appl. Catal.*, 1995, **126**, 333.
28 P. Vasudevan, N. Phougat and A. K. Shukla, *Appl. Organomet. Chem.*, 1996, **10**, 591.
29 J. H. Zagal, *Coord. Chem. Rev.*, 1992, **119**, 89.
30 F. Bedioui, J. Devynck and C. Bied-Charreton, *Acc. Chem. Res.*, 1995, **28**, 30.
31 B. Meunier, *Chem. Rev.*, 1992, **92**, 1411.
32 D. Mansuy, *Coord. Chem. Rev.*, 1993, **125**, 129.
33 F. Bedioui, *Coord. Chem. Rev.*, 1995, **144**, 39.
34 M. R. Tarasevich and K. A Radyushkina, *Russ. Chem. Rev.*, 1980, **49**, 718.
35 A. B. P. Lever, *J. Porph. Phthal.*, 1999, **3**, 488.
36 S. A. Wring, J. P. Hart and B. J. Birch, *Electroanalysis*, 1992, **4**, 299.
37 S. A. Wring and J. P. Hart, *Analyst*, 1992, **117**, 1281.
38 T. R. Ralph, M. L. Hitchman, J. P. Millington and F. C. Walsh, *J. Electroanal. Chem.*, 1994, **375**, 1.
39 Y.-H. Tse, P. Janda and A. B. P. Lever, *Anal. Chem.*, 1994, **66**, 384.
40 X. Qi and R. P. Baldwin, *Electroanalysis*, 1994, **6**, 353.
41 J. P. Hart and L. C. Hartley, *Analyst*, 1994, **119**, 259.
42 A. Napier and J. P. Hart, *Electroanalysis*, 1996, **8**, 1006.
43 T. J. Mafatle and T. Nyokong, *J. Electroanal. Chem.*, 1996, **408**, 213.
44 J. H. Zagal, M. Gulppi, C. Depretz and D. Leliévre, *J. Porphyr. Phthal.*, 1999, **3**, 355.
45 P. Ardiles, E. Trollund, M. Isaacs, F. Armijo and M. J. Aguirre, *J. Coord. Chem.*, 2001, **54**, 183.
46 R. O. Lezna, S. Juanto and J. H. Zagal, *J. Electroanal. Chem.*, 1998, **452**, 221.
47 J. H. Zagal, M. Gulppi, M. Isaacs, G. Cárdenas-Jirón and M. J. Aguirre, *Electrochim. Acta*, 1998, **44**, 1349.
48 D. Schlettwein and T. Yoshida, *J. Electroanal. Chem.*, 1998, **441**, 139.
49 J. H. Zagal, M. Gulppi, C. A. Caro and G. I. Cárdenas-Jirón, *Electrochem. Commun.*, 1999, **1**, 389.
50 G. I. Cárdenas-Jirón, M. A. Gulppi, C. A. Caro, R. Del Rio, M. Páez and J. H. Zagal, *Electrochim. Acta*, 2001, **46**, 3227.
51 S. Griveau, J. Pavez, J. H. Zagal and F. Bedioui, *J. Electroanal. Chem.*, 2001, **497**, 75.
52 S. Griveau, V. Albin, T. Pauporté, J. H. Zagal and F. Bedioui, *J. Mater. Chem.*, 2002, **12**, 225.
53 M. J. Aguirre, M. Isaacs, F. Armijo, L. Basáez and J. H. Zagal, *Electroanalysis*, 2002, **14**, 356.
54 M. Gulppi, S. Griveau, J. Pavez, J. H. Zagal and F. Bedioui, *Electroanalysis*, 2003, **15**, 779.
55 S. S. Khaloo, M. K. Amini, S. Tangestaninejad, S. Shahrokhian and R. Kia, *J. Iran. Chem. Soc.*, 2004, **1**, 128.
56 K. I. Ozoemena, T. Nyokong and P. Westbroek, *Electroanalysis*, 2003, **15**, 1762.
57 S. Shahrokhian and J. Yazdani, *Electrochim. Acta*, 2003, **48**, 4143.
58 S. Maree and T. Nyokong, *J. Electroanal. Chem.*, 2000, **492**, 120.
59 M. Sekota and T. Nyokong, *Electroanalysis*, 1997, **9**, 1257.
60 S. Shahrokhian, A. Hamzehloei, A. Thaghani and S. R. Mousavi, *Electroanalysis*, 2004, **16**, 915.
61 K. Ozoemena, P. Westbroek and T. Nyokong, *Electrochem. Commun.*, 2001, **3**, 529.
62 M. A. Gulppi, M. A. Páez, J. A. Costamagna, G. Cárdenas-Jirón, F. Bedioui and J. H. Zagal, *J. Electroanal. Chem.*, 2005, **580**, 50.
63 N. Sehlotho, T. Nyokong, J. H. Zagal and F. Bedioui, *Electrochim. Acta*, 2006, **51**, 5125.
64 J. H. Zagal, M. Gulppi and G. I. Cárdenas-Jirón, *Polyhedron*, 2000, **19**, 2255.
65 D. Geraldo, C. Linares, Y. Y. Chen, S. Ureta-Zañartu and J. H. Zagal, *Electrochem. Commun.*, 2002, **4**, 182.
66 C. Linares, D. Geraldo, M. Páez and J. H. Zagal, *J. Solid State Electrochem.*, 2003, **7**, 626.
67 S. Griveau, M. Gulppi, J. H. Zagal and F. Bedioui, *Solid State Ionics*, 2004, **169**, 59.
68 J. A. Claussen, G. Ochoa, M. Páez, J. Costamagna, T. Nyokong, F. Bedioui and J. H. Zagal, *J. Solid State Electrochem.*, in press.
69 J. E. Hutchison, T. A. Postlethwaite and R. W. Murray, *Langmuir*, 1993, **9**, 3277.
70 J. Zak, H. Yuan, M. Ho, L. K. Woo and M. D. Porter, *Langmuir*, 1993, **9**, 2772.
71 T. A. Postlethwaite, J. E. Hutchison, K. W. Hathcock and R. W. Murray, *Langmuir*, 1995, **11**, 4109.
72 M. J. Cook, *Pure Appl. Chem.*, 1999, **71**, 2145.
73 M. P. Somashekarappa, J. Keshavayya and S. Sampath, *Pure Appl. Chem.*, 2002, **74**, 1609.
74 M. P. Somashekarappa and S. Sampath, *Chem. Commun.*, 2002, 1262.
75 M. J. Cook, R. Hersans, J. McMurdo and D. A. Russell, *J. Mater. Chem.*, 1996, **6**, 149.
76 Z. Li and M. Lieberman, in *Fundamental and Applied Aspects of Chemically Modified Surfaces*, ed. J. P. Blitz and C. B. Little, Royal Society of Chemistry, Letchworth, 1999, pp. 24–35.
77 Z. Li, M. Lieberman and W. Hill, *Langmuir*, 2001, **17**, 4887.
78 T. Nyokong and F. Bedioui, *J. Porph. Phthal.*, 2006, **10**, 1101.
79 H. O. Finklea, in *Encyclopedia of Analytical Chemistry: Applications Theory and Instrumentations*, ed. R. A. Meyers, Wiley, 2000, ch. 11, pp. 10 090–10 116.
80 E. Salomon, T. Angot, N. Papageorgiou and J.-M. Layet, *Surf. Sci.*, 2005, **596**, 74.
81 M. Lackinger, T. Müller, T. G. Gopakumar, F. Müller, M. Hietschold and G. W. Flynn, *J. Phys. Chem. B*, 2004, **108**, 2279.
82 G. Kalyuzhny, A. Vaskevich, G. Ashkenasy, A. Shanzer and I. Rubinstein, *J. Phys. Chem. B*, 2000, **104**, 8238.
83 K. I. Ozoemena and T. Nyokong, *Talanta*, 2005, **67**, 162.
84 K. I. Ozoemena and T. Nyokong, *J. Electroanal. Chem.*, 2005, **579**, 283.
85 K. I. Ozoemena and T. Nyokong, *Electrochim. Acta*, 2006, **51**, 2669.
86 P. N. Mashazi, K. I. Ozoemena, D. M. Maree and T. Nyokong, *Electrochim. Acta*, 2006, **51**, 3489.
87 C. de la Fuente, J. A. Acuña, M. D. Vázquez, M. L. Tascón, M. I. Gómez and P. Sánchez Batanero, *Talanta*, 1997, **44**, 685.
88 T. Abe, T. Yoshida, S. Tokita, F. Taguchi, H. Imaya and M. Kaneko, *J. Electroanal. Chem.*, 1996, **412**, 125.
89 F. Zhao, J. Zhang, T. Abe, D. Wöhrle and M. Kaneko, *J. Mol. Catal. A: Chem.*, 1990, **145**, 245.
90 J. B. Zheng and Y. Wang, *Semicond. Photon. Tech.*, 2005, **11**, 94.
91 G. Muthuraman, Y.-B. Shim, J.-H. Yoon and M.-S. Won, *Synth. Met.*, 2005, **150**, 165.
92 H. Varela, R. L. Bruno and R. M. Torresi, *Polymer*, 2003, **44**, 5369.
93 A. Guadarrama, C. De la Fuente, J. A. Acuña, M. D. Vázquez, M. L. Tascón and P. Batanero, *Quim. Anal.*, 1999, **18**, 209.
94 S. Yagi, M. Kimura, T. Koyama, K. Hanabusa and H. Shirai, *Polym. J.*, 1995, **27**, 1139.
95 C. Coutanceau, A. El Hourch, P. Crouigneau, J. M. Léger and C. Lamy, *Electrochim. Acta*, 1995, **40**, 2739.
96 N. Inagaki, S. Tasaka and Y. Ikeda, *J. Appl. Polym. Sci.*, 1995, **55**, 1451.
97 H. Eichhorn, M. Sturm and D. Woehrle, *Macromol. Chem. Phys.*, 1995, **196**, 115.
98 J. R. Reynolds, M. Pyo and Y. J. Qiu, *J. Electrochem. Soc.*, 1994, **141**, 35.
99 A. El Hourch, A. Rakotondrainibe, B. Beden, P. Crouigneau, J. M. Léger, C. Lamy, A. A. Tanaka and E. R. González, *Electrochim. Acta*, 1994, **39**, 889.
100 A. El Hourch, S. Belcadi, P. Moisy, P. Crouigneau, J. M. Léger and C. Lamy, *J. Electroanal. Chem.*, 1992, **33**, 1.
101 M. Kawashima, Y. Sato, M. Sato and M. Sakaguchi, *Polym. J.*, 1991, **23**, 37.

102 R. A. Bull, F. R. Fan and A. J. Bard, *J. Electrochem. Soc.*, 1984, **131**, 687.
103 M. Kimura, T. Horai, K. Hanabusa and H. Shirai, *Chem. Lett.*, 1997, **7**, 653.
104 Y. J. Qui and J. R. Reynolds, *J. Polym. Sci., Part A: Polym. Chem.*, 1992, **30**, 1315.
105 S. Kurosawa, E. Tawara-Kondo, N. Minoura and N. Kamo, *Sensors Actuators, B: Chem.*, 1997, **43**, 175.
106 S. Kurosawa, E. Tawara-Kondo and N. Kamo, *Anal. Chim. Acta*, 1997, **337**, 1.
107 A. Yu, W. Xu, W. Yang and Q. Jin, *Chin. Chem. Lett.*, 1991, **2**, 879.
108 Y. Osada and A. Mizumoto, *J. Appl. Phys.*, 1986, **59**, 1776.
109 A. Ferencz, N. R. Armstrong and G. Wegner, *Macromolecules*, 1994, **27**, 1517.
110 A. Pailleret and F. Bedioui, in *N4-Macrocyclic Metal Complexes*, ed. J. H. Zagal, F. Bedioui and J. P. Dodelet, Springer, New York, 2006, p. 363.
111 *Electrochemical Science and Technology of polymers*, ed. R. G. Linford, Elsevier, London and New York, 1987.
112 J. Heinze, *Top. Curr. Chem.*, 1990, **152**, 1.
113 A. Merz, *Top. Curr. Chem.*, 1990, **152**, 49.
114 *Handbook of Conducting Polymers*, ed. T. A. Skotheim, Marcel Dekker, New York, vol. 1 and 2, 1986.
115 A. Deronzier and J. C. Moutet, *Acc. Chem. Res.*, 1989, **22**, 249.
116 D. Curran, J. Grimshaw and S. D. Perera, *Chem. Soc. Rev.*, 1991, **20**, 391.
117 J. Roncali, *Chem. Rev.*, 1992, **92**, 711.
118 E. M. Bruti, M. Giannetto, G. Mori and R. Seeber, *Electroanalysis*, 1999, **11**, 565.
119 K. Okabayashi, O. Ikeda and H. Tamura, *J. Chem. Soc., Chem. Commun.*, 1983, 684.
120 F. Bedioui, C. Bongars, C. Hinnen, C. Bied-Charreton and J. Devynck, *Bull. Soc. Chim. Fr.*, 1985, 679.
121 O. Ikeda, K. Okabayshi, N. Yoshida and H. Tamura, *J. Electroanal. Chem.*, 1985, **191**, 157.
122 F. Bedioui, C. Bongars, J. Devynck, C. Bied-Charreton and C. Hinnen, *J. Electroanal. Chem.*, 1986, **207**, 87.
123 T. Skotheim, M. Velasquez Rosenthal and C. A. Linkous, *J. Chem. Soc., Chem. Commun.*, 1985, 612.
124 F. Mizutani, S. I. Lijima, Y. Tanabe and K. Tsuda, *J. Chem. Soc., Chem. Commun.*, 1985, 1728.
125 M. Velasquez Rosenthal, T. A. Skotheim and C. A. Linkous, *Synth. Met.*, 1986, **15**, 219.
126 A. Elzing, A. Van der Putten, W. Visscher and E. Barendrecht, *J. Electroanal. Chem.*, 1987, **233**, 113.
127 R. Jiang and S. Dong, *J. Electroanal. Chem.*, 1988, **246**, 101.
128 C. S. Choi and H. Tachikawa, *J. Am. Chem. Soc.*, 1990, **112**, 1757.
129 D. J. Walton, D. M. Hadingham, C. E. Hall, I. V. F. Viney and A. Chyla, *Synth. Met.*, 1991, **41**, 295.
130 B. R. Saunders, K. S. Murray and R. J. Fleming, *Synth. Met.*, 1992, **47**, 167.
131 N. Trombach, O. Hild, D. Schlettwein and D. Wöhrle, *J. Mater. Chem.*, 2002, **12**, 879.
132 D. Wöhrle, O. Hild, N. Trombach, R. Benters, G. Schnurpfeil and O. Suvorova, *Macromol. Symp.*, 2002, **186**, 99.
133 J. Obirai, N. Pereira Rodrigues, F. Bedioui and T. Nyokong, *J. Porph. Phthal.*, 2003, **7**, 508.
134 J. Obirai and T. Nyokong, *J. Electroanal. Chem.*, 2004, **57**, 77.
135 K. L. Brown, J. Shaw, M. Ambrose and H. A. Mottola, *Microchemical Journal*, 2002, **72**, 285.
136 E. Trollund, P. Ardiles, M. J. Aguirre, S. R. Biaggio and R. C. Rocha-Filho, *Polyhedron*, 2000, **19**, 2303.
137 S. Zhang, W.-L. Sun, Y.-Z. Xian, W. Zhang, L.-T. Jin, K. Yamamoto, S. Tao and J. Jin, *Anal. Chim. Acta*, 1999, **399**, 213.
138 M. E. Boyle, J. D. Adkins, A. W. Snow, R. F. Cozzens and R. F. Brady, Jr, *J. Appl. Polym. Sci.*, 1995, **57**, 77.
139 J. Wang, *Anal. Lett.*, 1996, **29**, 1575.
140 G. Ramirez, E. Trollund, J. C. Canales, M. J. Canales, F. Armijo and M. J. Aguirre, *Bol. Soc. Chil. Quim.*, 2001, **46**, 247.
141 N. M. Alpatova, E. V. Ovsyannikova, L. G. Tomilova, O. V. Korenchenko and Y. Kondrashov, *Russ. J. Electrochem.*, 2001, **37**, 1012.
142 T. V. Magdesieva, I. V. Zhukov, D. N. Kravchuk, O. A. Semenikhin, L. G. Tomilova and K. P. Butin, *Russ. Chem. Bull.*, 2002, **51**, 805.
143 K. L. Brown and H. A. Mottola, *Langmuir*, 1998, **14**, 3411.
144 Y. H. Tse, P. Janda, H. Lam and A. B. P. Lever, *Anal. Chem.*, 1995, **67**, 981.
145 J. Obirai and T. Nyokong, *Electrochim. Acta*, 2004, **49**, 1417.
146 G. Ramírez, E. Trollund, M. Isaacs, F. Armijo, J. Zagal, J. Costamagna and M. J. Aguirre, *Electroanalysis*, 2002, **14**, 540.
147 A. Goux, F. Bedioui, L. Robbiola and M. Pontié, *Electroanalysis*, 2003, **15**, 969.
148 N. Pereira Rodrigues, J. Obirai, T. Nyokong and F. Bedioui, *Electroanalysis*, 2005, **17**, 186.
149 P. Janda, J. Weber, L. Dunsch and A. B. P. Lever, *Anal. Chem.*, 1996, **68**, 960.
150 J. H. Zagal and C. Páez, *Electrochim. Acta*, 1989, **34**, 243.
151 J. H. Zagal, P. Herrera, K. Brinck and S. Ureta-Zañartu, *Proc. Electrochem. Soc.*, 1984, **84**, 602.
152 M. K. Halbert and R. P. Baldwin, *Anal. Chem.*, 1985, **57**, 591.
153 J. Telesford and P. D. Voegel, Abstracts 230th ACS National Meeting, Washington DC, Aug. 28–Sept. 1, 2005, CHED-139.
154 P. D. Voegel and J. Telesford, 60th Southwest regional meeting of ACS, Fort Worth, Texas, Sept. 29–Oct. 4, 2004, SEPT04-315.
155 J. H. Zagal, M. E. Vaschetto and B. A. Retamal, *Int. J. Polym. Mater.*, 1999, **44**, 225.
156 S. A. Wring, J. P. Hart and B. J. Birch, *Talanta*, 1991, **38**, 1257.
157 L. G. Popesku, L. G. Shaidarova and G. K. Budnikov, *Ind. Lab. (Diagnostic Mater.)*, 1999, **65**, 423.
158 P. Vasudevan, N. Phougat and A. K. Shukla, *Appl. Organomet. Chem.*, 1996, **10**, 591.
159 J. H. Zagal and P. Herrera, *Electrochim. Acta*, 1985, **30**, 449.
160 A. J. Appleby, in *Modern Aspects of Electrochemistry*, ed. B. Conway and J. O'M. Bockris, Plenum Press, vol. 9, 1974, p. 369.
161 T. Bligaard, J. K. Nørskov, S. Dahl, J. Matthiesen, C. H. Christensen and J. Sehested, *J. Catal.*, 2004, **224**, 206.
162 B. E. Conway and J. Jerkiewicz, *Electrochim. Acta*, 2000, **45**, 4075.
163 R. Parsons, *Trans. Faraday Soc.*, 1958, **54**, 1053.
164 R. Parsons, *Surf. Sci.*, 1964, **2**, 418.
165 R. Parsons, *Surf. Sci.*, 1969, **18**, 28.
166 S. Trasatti, *J. Electroanal. Chem.*, 1971, **33**, 351.
167 S. Trasatti, *J. Electroanal. Chem.*, 1972, **39**, 163.
168 S. Trasatti, in *Advances in Electrochemistry and Electrochemical Engineering*, ed. C.W. Tobias and H. Gerischer, Interscience, New York, 1977, vol. 10, p. 213.
169 S. Trasatti, in *Proceedings of the Symposium on Electrocatalysis*, ed. W. E. O'Grady, P. N. Ross and F. G. Will, The Electrochemical Society Proceeding Series, Pennington NJ, 1982, p.73.
170 J. H. Zagal, M. Páez and J. F. Silva, in *N4-Macrocyclic Metal Complexes*, ed. J. H. Zagal, F. Bedioui and J. P. Dodelet, Springer, New York, 2006, p. 55.
171 A. Rosa and E. J. Baerends, *Inorg. Chem.*, 1994, **33**, 584.
172 K. W. Hipps, X. Lung, X. D. Wang and U. Manzur, *J. Phys. Chem. B*, 1996, **100**, 11207.
173 H. Gerischer, *Z. Phys. Chem. N. F.*, 1956, **8**, 137.
174 J. O'M. Bockris and A. K. M. Reddy, in *Modern Electrochemistry*, vol. 2, first edn, Plenum Press, New York, 1997, pp. 960–981.
175 J. M. Jaksic, N. M. Ristic, N. V. Krstajic and M. M. Jaksic, *Int. J. Hydrogen Energy*, 1998, **23**, 1121.
176 M. M. Jaksic, *Electrochim. Acta*, 2000, **45**, 4085.
177 M. M. Jaksic, *Int. J. Hydrogen Energy*, 2001, **26**, 559.
178 M. M. Jaksic, *Solid State Ionics*, 2000, **136–137**, 733.

